Conceptual Design Report
The Neutrino Experiment

Volume w: LBNF/DUNE Physics

April 9, 2015

1

Contents

2

List of Figures

5

List of Tables

1

Todo list

Chapter 1

Overview

ysics-overview

Chapter 2

LBNE/Dune Scientific Goals

:physics-goals

Chapter 3

Long-baseline Neutrino Oscillation Physics

3.1 Context

3.2 Mass Hierarchy

3.3 CP-symmetry Violation

3.4 Testing the 3-flavour Paradigm

3.5 Neutrino Beam Requirements

3.6 Far Detector Requirements

3.7 Beam systematic errors and Near Detector Requirements

Chapter 4

Nucleon Decay and Atmospheric Neutrinos

4.1 Nucleon Decay

4.1.1 Physics Motivation

The class of theories known as Grand Unified Theories (GUTs) make predictions about both baryon number violation and proton lifetime that may be within reach of the full-scope DUNE experiment. The theoretical motivation for the study of proton decay has a long and distinguished history [?, ?, ?] and has been reviewed many times [?, ?, ?]. Early GUTs provided the original motivation for proton decay searches in kiloton-scale detectors placed deep underground to limit backgrounds. The 22.5-kt Super–Kamiokande experiment extended the search for proton decay by more than an order of magnitude relative to the previous generation of experiments. Contemporary reviews [?, ?, ?] discuss the strict limits already set by Super–Kamiokande and the context of the proposed next generation of larger underground experiments such as Hyper-Kamiokande and DUNE.

Although no evidence for proton decay has been detected, the lifetime limits from the current generation of experiments already constrain the construction of many contemporary GUT models. In some cases, these lifetime limits are approaching the upper limits allowed by GUT models. This situation points naturally toward continuing the search with new, larger detectors.

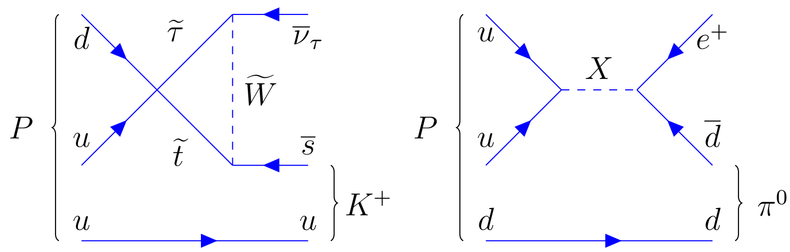

Figure 4.1: Feynman diagrams for proton decay modes from supersymmetric GUT, $p^+ \to K^+\overline{\nu}$ (left) and gauge-mediation GUT models, $p^+ \to e^+\pi^0$ (right).

4.1.2 Proton Decay Modes

From the body of literature, two decay modes (shown in Figure 4.1) emerge that dominate the DUNE experimental design. The more well-known of the two, the decay mode of $p \to e^+\pi^0$, arises from gauge mediation. It is often predicted to have the higher branching fraction and is also demonstrably the more straightforward experimental signature for a water Cherenkov detector. In this mode, the total mass of the proton is converted into the electromagnetic shower energy of the positron and two photons from π^0 decay, with a net momentum vector near zero.

The second key mode is $p \to K^+\overline{\nu}$. This mode is dominant in most supersymmetric GUTs, many of which also favor additional modes involving kaons in the final state. This decay mode with a charged kaon is uniquely interesting; since stopping kaons have a higher ionization density than other particles, a LArTPC could detect it with extremely high efficiency. In addition, many final states of K^+ decay would be fully reconstructable in a LArTPC.

There are many other allowed modes of proton or bound neutron into antilepton plus meson decay that conserve $B - L$[1]. Other modes that conserve $B + L$, or that decay only into leptons, have also been hypothesized. These possibilities are less well-motivated theoretically, as they do not appear in a wide range of models, and are therefore not considered here.

Figure **??** shows a comparison of experimental limits, dominated by recent results from Super–Kamiokande to the ranges of lifetimes predicted by an assortment of GUTs. At this time, the theory literature does not attempt to precisely predict lifetimes, concentrating instead on suggesting the dominant decay modes and relative branching ratios. The uncertainty in the lifetime predictions comes from details of

[1] In these models, the quantum number $B - L$ is expected to be conserved even though B and L are not individually conserved.

the theory, such as masses and coupling constants of unknown heavy particles, as well as poorly known details of matrix elements for quarks within the nucleon.

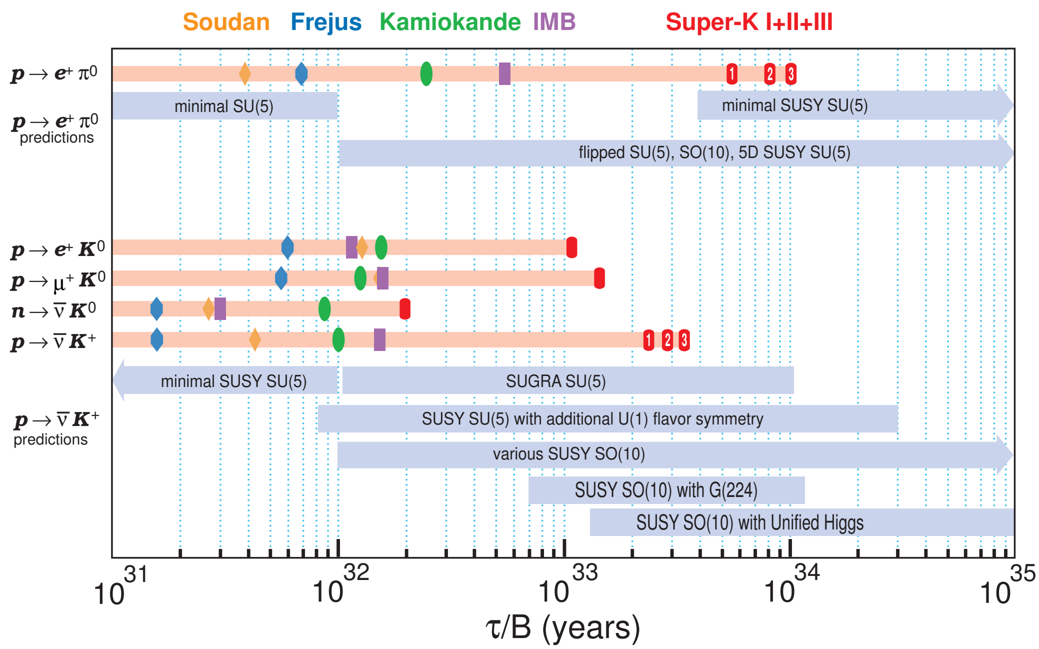

Figure 4.2: Proton decay lifetime limits [?, ?] compared to lifetime ranges predicted by Grand Unified Theories. The upper section is for $p \to e^+\pi^0$, most commonly caused by gauge mediation. The lower section is for SUSY-motivated models, which commonly predict decay modes with kaons in the final state. The marker symbols indicate published experimental limits, as indicated by the sequence and colors on top of the figure.

It is apparent from Figure **??** that a continued search for proton decay is by no means assured of obtaining a positive result. With that caveat, an experiment with sensitivity to proton lifetimes between 10^{33} and 10^{35} years is searching in the right territory over virtually all GUTs; even if no proton decay is detected, stringent lifetime limits will provide strong constraints on such models. Minimal SU(5) was ruled out by the early work of IMB and Kamiokande and minimal SUSY SU(5) is considered to be ruled out by Super–Kamiokande. In most cases, another order of magnitude in improved limits will not rule out specific models but will constrain their allowed parameters; this could allow identification of models which must be fine-tuned in order to accommodate the data, and are thus less favored.

4.1.3 Signatures for Nucleon Decay in Liquid Argon

For modes with no electron in the final state, the same displaced vertex performance that underpins long-baseline neutrino oscillation measurements allows the rejection of CC interactions of atmospheric ν_e's. As will be stressed for the key mode of $p \to K^+\overline{\nu}$ described in detail below, the capability to reconstruct the charged kaon with the proper range and dE/dx profile allows for a high-efficiency, background-free analysis. In general, these criteria favor all modes with a kaon, charged or neutral, in the final state. Conversely, the efficiency for decay modes to a lepton plus light meson will be limited by intranuclear reactions that plague liquid argon to a greater extent than they do ^{16}O in a water Cherenkov detector.

An extensive survey [**?**] of nucleon decay efficiency and background rates for large LArTPCs with various depth/overburden conditions, published in 2007, provides the starting point for the assessment of DUNE's capabilities. Table 4.2 lists selected modes where LArTPC technology exhibits a significant performance advantage (per kiloton) over the water Cherenkov technology. The remainder of this chapter focuses on the capabilities of DUNE for the $p \to K^+\overline{\nu}$ channel, as the most promising from theoretical and experimental considerations. Much of the discussion that follows can be applied to cover the other channels with kaons listed in the table.

Table 4.1: Efficiencies and background rates (events per Mt · year) for nucleon decay channels of interest for a large underground LArTPC [**?**], and comparison with water Cherenkov detector capabilities. The entries for the water Cherenkov capabilities are based on experience with the Super–Kamiokande detector [**?**].

Decay Mode	Water Cherenkov		Liquid Argon TPC	
	Efficiency	Background	Efficiency	Background
$p \to K^+\overline{\nu}$	19%	4	97%	1
$p \to K^0\mu^+$	10%	8	47%	< 2
$p \to K^+\mu^-\pi^+$			97%	1
$n \to K^+e^-$	10%	3	96%	< 2
$n \to e^+\pi^-$	19%	2	44%	0.8

The key signature for $p \to K^+\overline{\nu}$ is the presence of an isolated charged kaon (which would also be monochromatic for the case of free protons, with p =340 MeV). Unlike the case of $p \to e^+\pi^0$, where the maximum detection efficiency is limited to 40–45% because of inelastic intranuclear scattering of the π^0, the kaon in $p \to K^+\overline{\nu}$ emerges intact (because the kaon momentum is below threshold for inelastic reactions) from the nuclear environment of the decaying proton $\sim$ 97% of the time. Nuclear effects come into play in other ways, however: the kaon momentum is smeared by the proton's Fermi motion and shifted downward by re-scattering [**?**]. Not all K decay modes are reconstructable, however, and even for those that are, insufficient information exists to determine the initial K momentum. Still, water detectors can reconstruct significant hadronic channels such as $K^+ \to \pi^+\pi^0$ decay, and the 6-MeV gamma from de-excitation of O^{16} provides an added signature to help with the $K^+ \to \mu^+\nu$ channel. The overall detection efficiency in SK [**?**] thus approaches 20%.

In LArTPC detectors, the K^+ can be tracked, its momentum measured by range, and its identity positively resolved via detailed analysis of its energy-loss profile. Additionally, all decay modes can be cleanly reconstructed and identified, including those with neutrinos, since the decaying proton is essentially at rest. With this level of detail, it is possible for a single event to provide overwhelming evidence for the appearance of an isolated kaon of the right momentum originating from a point within the fiducial volume. The strength of this signature is clear from cosmogenic-induced kaons observed by the ICARUS Collaboration in the cosmic-ray (CR) test run of half of the T600 detector, performed at a surface installation in Pavia [**?**] and in high-energy neutrino interactions with the full T600 in the recent CNGS (CERN Neutrinos to Gran Sasso) run [**?**]. Figure 4.3 shows a sample event from the CNGS run in which the kaon is observed as a progressively heavily-ionizing track that crosses into the active liquid argon volume, stops, and decays to $\mu\nu$, producing a muon track that also stops and decays such that the Michel-electron track is also visible.

If it can be demonstrated that background processes mimicking this signature can be rejected at the appropriate level, a single $p \to K^+\overline{\nu}$ candidate could constitute evidence for proton decay.

Ref. [**?**] presented a detailed examination of possible backgrounds, including those arising from cosmic ray interactions in the detector and surrounding rock, atmospheric neutrino interactions in the dectector, and reconstruction failiures. Table **??** summarizes the results of those background studies.

4.1.4 Summary of Expected Sensitivity to Key Nucleon Decay Modes

Based on the expected signal efficiency and the upper limit on the background rates estimated in Section **??**, the expected limit on the proton lifetime as a function of running time in DUNE for $p \to K^+\overline{\nu}$ is shown in Figure 4.4. Figure 4.4 demonstrates

Table 4.2: Background rates (events per Mt · year) for nucleon decay

Background Source	Mitigation Strategy	Leakage Rate (events per Mt · year)
Internal cosmic ray spallation	Energy threshold	Negligible
External cosmogenic K^+ production	Depth, fiducialization	Negligible
External cosmogenic K^0 production +internal charge-exchange to K^+	Cuts on other secondaries	2
Atmospheric ν $\Delta S = 0$ processes	Cut on associated strange baryon	Negligible
Atmospheric ν $\Delta S = 1$ processes	Cabibo-suppressed, lepton ID	Negligible
Atmospheric ν with π mis-ID	dE/dx discrimination, +236 MeV muon track	Negligible
Reconstruction pathologies	dE/dx profiles vs track length	Negligible

tab:pdecay

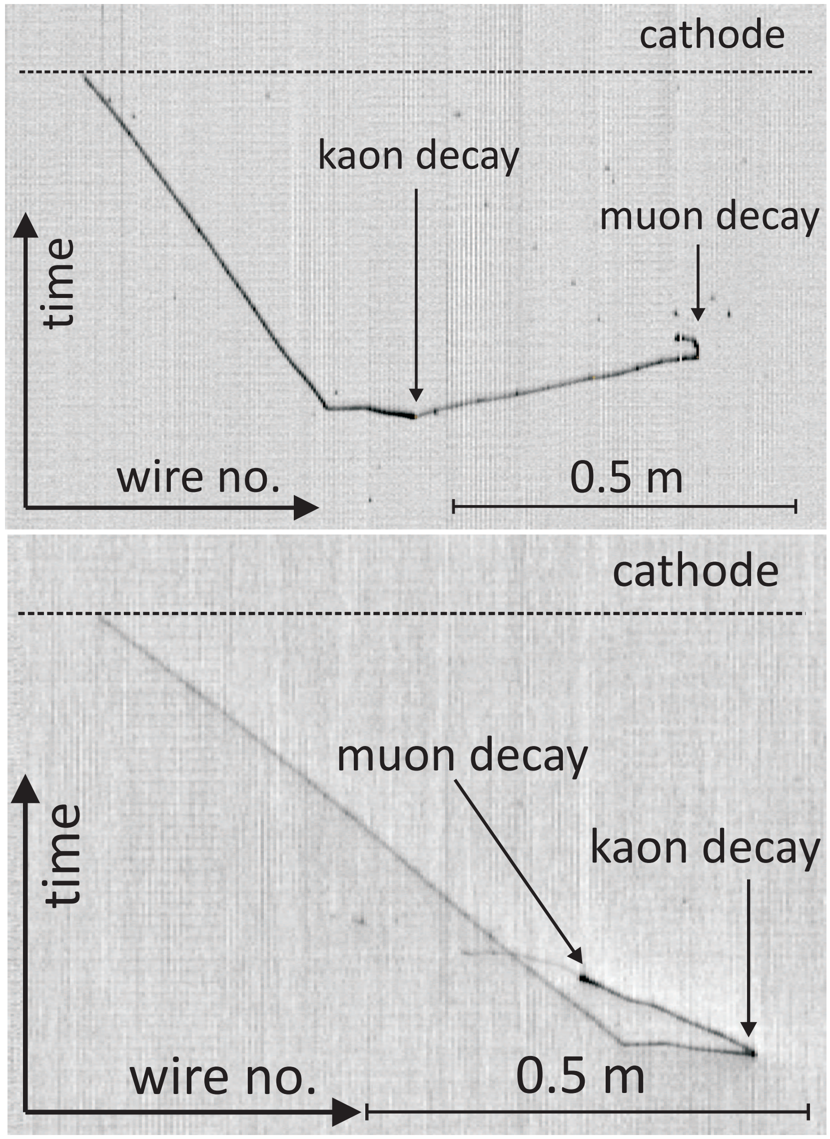

Figure 4.3: Event display for a decaying kaon candidate $K \rightarrow \mu\nu_{\mu}$ $\mu \rightarrow e\nu_{e}\nu_{\mu}$ in the ICARUS T600 detector observed in the CNGS data (K: 90 cm, 325 MeV; μ : 54 cm, 147 MeV; e : 13 cm, 27 MeV). The top figure shows the signal on the collection plane, and the bottom figure shows the signal on the second induction plane [**?**]. Antonello:2012hu fig:icaruskaon

that to improve the current limits on the $p \rightarrow \overline{\nu}K^{+}$, set by Super–Kamiokande, significantly beyond that experiment's sensitivity, a LArTPC detector of at least

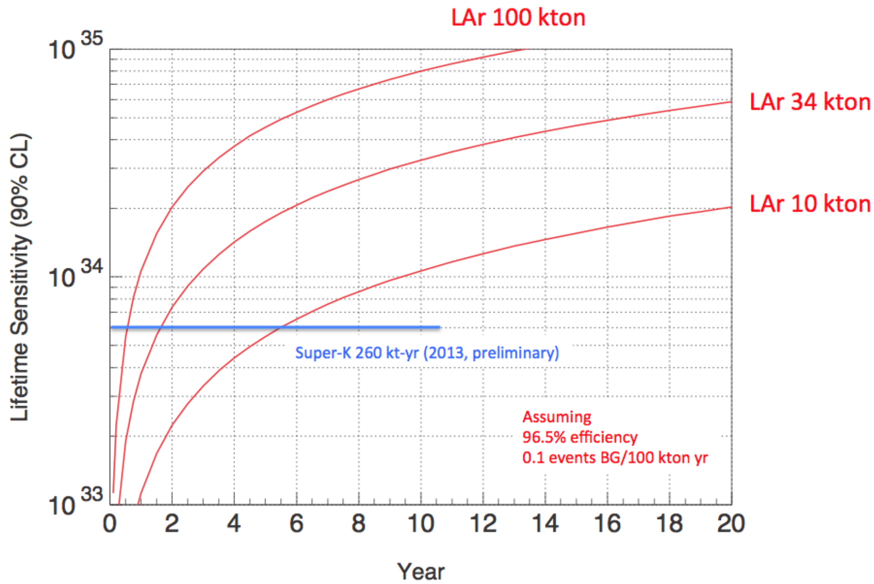

Figure 4.4: Proton decay lifetime limit for $p \to K^+\overline{\nu}$ as a function of time for underground LArTPCs of fiducial masses 10, 34 and 100 kt. For comparison, the current limit from SK is also shown. The limits are at 90% C.L., calculated for a Poisson process including background, assuming that the detected events equal the expected background.

10 kt, installed deep underground, is needed. A 34-kt detector will improve the current limits by an order of magnitude after running for two decades. Clearly a larger detector mass would improve the limits even more in that span of time.

While the background rates are thought to be no higher than those assumed in generating the above sensitivity projections, it is possible to estimate the impact of higher rates. For $p \to K^+\overline{\nu}$, Table 4.3 shows a comparison of the 90% CL lower bounds on proton lifetime for an exposure of $340\,\mathrm{kt}\cdot\mathrm{year}$ assuming the nominal 1.0 per $\mathrm{Mt}\cdot\mathrm{year}$ background rate with the corresponding bounds for a rate that is ten times higher, as well as for a fully background-free experiment. While a factor of ten increase in the background would hurt the sensitivity, useful limits can still be obtained. As stated above, however, there is good reason to believe such a case is highly unlikely.

Sensitivities have been computed for some of the other decay channels listed in Table 4.2. The limits that could be obtained from an DUNE 34-kt detector in ten years of running as compared to other proposed future experiments and theoretical expectations are shown in Figure 4.5.

Table 4.3: The impact of different assumed background rates on the expected 90% CL lower bound for the partial proton lifetime for the $p \to K^+\overline{\nu}$ channel, for a 34-kt detector operating for ten years. The expected background rate is one event per Mt · year. Systematic uncertainties are not included in these evaluations.

ay-bgvariation

Background Rate	Expected Partial Lifetime Limit
0 events/Mt · year	3.8×10^{34} years
1 events/Mt · year	3.3×10^{34} years
10 events/Mt · year	2.0×10^{34} years

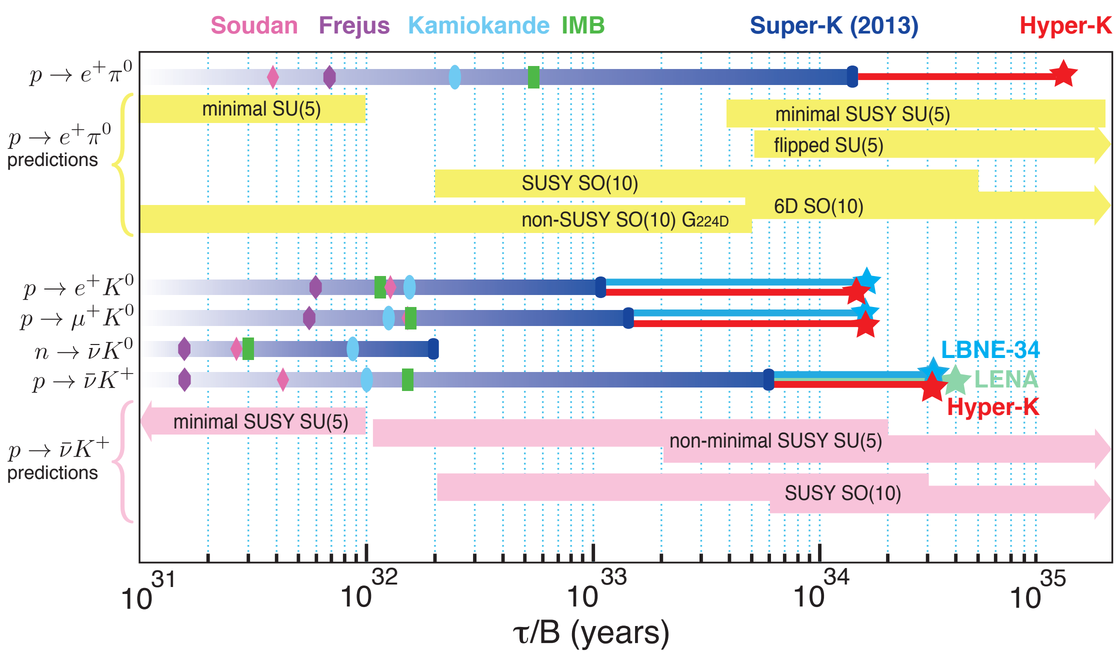

Figure 4.5: Proton decay lifetime limits that can be achieved by the DUNE 34-kt detector compared to other proposed future experiments. The limits are at 90% C.L., calculated for a Poisson process including background, assuming that the detected events equal the expected background.

fig:nnn13

4.2 Atmospheric Neutrinos

s-atmpdk-atmnu

4.3 Detector Requirements

r-requirements

Chapter 5

Supernova Neutrino Bursts and Low-energy Neutrinos

5.1 Overview

5.2 Neutrino Physics

5.3 Astrophysics

5.4 Detector Requirements

5.5 Additional Astrophysical Neutrinos

Chapter 6

Near Detector Physics

ch:physics-nd

Chapter 7

Summary of Physics

hysics-summary